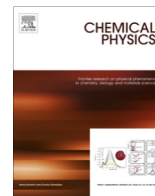




Contents lists available at ScienceDirect

Chemical Physics

journal homepage: www.elsevier.com/locate/chemphys

Dynamic interference in the resonance-enhanced multiphoton ionization of hydrogen atoms by short and intense laser pulses

Anne D. Müller^a, Eric Kutscher^a, Anton N. Artemyev^a, Lorenz S. Cederbaum^b, Philipp V. Demekhin^{a,*}

^a Institut für Physik und CINSaT, Universität Kassel, Heinrich-Plett-Str. 40, 34132 Kassel, Germany

^b Theoretische Chemie, Physikalisch-Chemisches Institut, Universität Heidelberg, Im Neuenheimer Feld 229, 69120 Heidelberg, Germany

ARTICLE INFO

Article history:

Received 7 September 2017

In final form 19 October 2017

Available online xxx

Keywords:

Spectra induced by intense laser pulses

Multiphoton ionization and excitation

Photoinduced electron dynamics

ABSTRACT

Photoionization of the hydrogen atom by intense and short coherent laser pulses is investigated from first principles by a numerical solution of the time-dependent Schrödinger equation in the dipole-velocity gauge. The considered photon energies are resonant to the $1s \rightarrow 2p$ excitation, and the pulse intensities are high enough to induce Rabi floppings. The computed resonance-enhanced two-photon ionization spectra as well as the three-photon above threshold ionization spectra exhibit pronounced multiple-peak patterns due to dynamic interference. Fingerprints of dynamic interference can also be seen directly in the radial density of the photoelectron. The impact of the variation of the pulse intensity and photon energy on the dynamic interference is investigated, and the angular distribution of the emitted electrons is analyzed in some details. The present precise numerical results confirm our previous theoretical predictions on the two-photon ionization spectra (Demekhin and Cederbaum, 2012) made within a minimal few-level model.

© 2017 Elsevier B.V. All rights reserved.

1. Introduction

With the advent of new techniques to generate intense and short X-ray laser pulses [1–5], new aspects of light-matter interaction can be studied. One of the fundamental phenomena emerging in this field regime is known as dynamic interference [6,7]. Here, the strong pulse couples different states and causes thereby an AC-Stark shift or Autler-Towns energy splitting. If the pulse supports many optical cycles, this splitting follows the time-envelope of the pulse [8]. Because of energy conservation, the emitted photoelectrons have different kinetic energies, depending on when they were released. The photoelectron wave packets of the same kinetic energy emitted at different times along the pulse superimpose. This results in interference structures in the electron spectrum around the energy which is expected in the weak-field limit. This phenomenon can be understood as a double-slit interference in the time domain [6,7,9].

The dynamic interference was already studied theoretically for several systems and scenarios using different methods [6,7,9–15]. In Refs. [6,9,10], the photoionization (PI) of hydrogen atoms by intense laser pulses was studied by a minimal few-level model. A similar model was applied to investigate the dynamic interference

in the resonant Auger decay of neon [9,11] and xenon [12] atoms. Calculations of the PI and above threshold ionization (ATI) of model anions were conducted in Refs. [13,14] in the Kramers-Henneberger frame. The dynamic interference in the PI of hydrogen was reinvestigated more precisely in Ref. [7] by a direct propagation of one-electron wave packets and found to appear in the PI from an excited state. Particularly amenable to experiments is the detection of dynamic interference in the PI of helium (see supplementary material in Ref. [6]) which is reinvestigated theoretically in Ref. [15] by the direct propagation of the corresponding two-electron wave packets.

In our previous work in Ref. [9], the dynamic interference in the resonance-enhanced two-photon ionization of hydrogen was investigated using a minimal few-level model. Here, a coherent resonant laser pulse couples the $1s$ ground and $2p$ excited states of hydrogen. In the adiabatic picture, the resulting two states repel each other and split in energy. This superposition of the coupled dressed states is probed by a second photon from the same pulse. Because of the pulse-envelope, the energy splitting and hence the kinetic energy of the emitted electrons change in time, resulting in dynamic interference. This process is schematically illustrated in Fig. 4 of Ref. [9]. Our previous work predicts a very rich multiple-peak structure in the electron spectrum, the complexity of which grows with the pulse intensity. However, the theoretical model implemented in Ref. [9] is restricted to low-order photon

* Corresponding author.

E-mail address: demekhin@physik.uni-kassel.de (P.V. Demekhin).

absorption processes and neglects the manifold of highly-excited states. In order to verify the predictions of Ref. [9], we reinvestigate here this process numerically exactly, by solving the time-dependent Schrödinger equation (TDSE). Moreover, we extend the investigation and compute and analyze also the above threshold ionization spectrum, the angular distribution of the emitted electrons and the impact of dynamic interference on the radial density of the emitted photoelectrons.

At present, solving numerically the TDSE for one-electron atoms in intense laser fields is a rather common task [7,16–32]. For instance, the propagation of the one-electron wave packets in hydrogen-like atoms has been successfully realized by many groups in order to investigate direct ionization by high-frequency intense pulses [7,16–20], as well as to study strong-field tunnel ionization and high order harmonic generation [21–24] by infrared pulses. For larger atoms, a single-active-electron approximation [25,26] or even direct propagation of correlated multi-electron wave packets by different methods [27–32] have been reported. In addition, different realizations of the Floquet technique have been successfully applied in many studies of multiphoton and above threshold ionization of atomic hydrogen [33–36].

Here, we utilize the theoretical approach developed in our previous works in Refs. [15,37–40], which was successfully applied to propagate one-electron wave packets in hydrogen [37], single-active-electron wave packets in model chiral systems [38], and also two-electron wave packets in helium [15,39,40]. The paper is organized as follows. In Section 2, we outline the essential points of how we solve numerically the TDSE for hydrogen atom. The numerical results obtained on the dynamic interference are presented and discussed in Section 3. We conclude in Section 4 with a brief summary.

2. Computational method

The TDSE for the hydrogen atom in the field of a linearly polarized laser pulse reads (atomic units used throughout):

$$i \frac{\partial \Psi(\vec{r}, t)}{\partial t} = \left(-\frac{1}{2} \nabla^2 - \frac{1}{r} - i \nabla_z A_0 g(t) \sin(\omega t) \right) \Psi(\vec{r}, t). \quad (1)$$

Here, ω is the carrier frequency of the pulse and $g(t)$ its time-envelope. The peak intensity I_0 is defined as $I_0 = \frac{\omega^2}{8\pi\alpha} A_0^2$, with α being the fine-structure constant and A_0 the peak amplitude of the vector potential. Eq. (1) describes the light-matter interaction in the dipole-velocity gauge, which is most suitable for the numerical treatment of strong-field problems [41,42].

To solve the TDSE (1) numerically we used the theoretical method and computer code developed in our previous works [15,37–40]. Here, the one-electron wave function $\Psi(\vec{r}, t)$ is expanded in terms of partial waves via spherical harmonics. The radial coordinate is represented by a finite-element discrete-variable representation. Each finite element is covered by normalized Lagrange interpolating polynomials, which are constructed over a Gauss-Lobatto grid [43–45]. With this finite-element discrete-variable representation, the matrix elements of the Hamiltonian in Eq. (1) can be evaluated analytically (see Refs. [15,37–40] for explicit expressions).

The time-dependent electron wave packet was propagated using the short-iterative Lanczos method [46]. The initial state of the propagation, i.e., the ground state of the hydrogen atom, was found by imaginary time propagation, i.e., by the relaxation from an arbitrary guess function. In order to prevent reflection of the wave packet from the grid boundary, a mask function [39,40] was applied at the end of the grid. After the propagation, the final spatial wave packet $\Psi(\vec{r}, t = \infty)$ contains the complete information

on the momentum distribution of the emitted photoelectron, which is determined by its Fourier transformation to $\Psi(\vec{k})$. To ensure that bound electrons do not contribute to the emission spectrum, the inner part of the wave packet was excluded from this transformation.

In the calculations, all parameters of the pulse were chosen in accordance with Ref. [9]. In particular, we used linearly polarized Gaussian-shaped pulses of $\tau = 30$ fs duration. The carrier frequency $\omega = 0.375$ a.u. is chosen to be equal to the $1s \rightarrow 2p$ excitation energy. We also performed computations varying this value. Calculations were performed for those peak intensities which enable the completion of an integer number of Rabi cycles between the coupled electronic states during the pulse (see also Fig. 1 in Ref. [9]). To observe dynamic interference in the PI and ATI spectra, it is necessary to propagate the full electron wave packet during the entire pulse duration. For a Gaussian-shaped pulse, propagating during the time-interval of $\pm 3\tau$ around its maximum is sufficient to describe the processes. The electrons released by the three-photon ATI process have a momentum of about $k \sim 1.2$ a.u. and can move during this propagation time by a distance of about 10000 a.u., which was chosen to be the radial grid size. The grid was divided into 5000 finite elements of length 2 a.u., each supporting 10 Gauss-Lobatto points. The partial wave expansion of the photoelectron wave packet was restricted to $\ell \leq 5$, which was found to ensure the convergence of the numerical solutions over the angular momentum.

3. Results and discussion

We first discuss the computational results obtained for the carrier frequency of $\omega = 0.375$ a.u. The final radial densities of the photoelectron wave packets, computed for different peak intensities (indicated on the left of each curve), are depicted in Fig. 1. For the lowest considered intensity (lowermost curve in the figure), two major features are observable in the radial wave packet. The hump at around 2500 a.u. describes the slow PI electrons with kinetic energy of about $\epsilon_{PI}^0 = 2\omega - IP$ (where IP denotes the ionization potential of hydrogen atom). The somewhat weaker shoulder at around 4500 a.u., which partly overlaps with the hump, represents the faster ATI electrons having kinetic energy of about $\epsilon_{ATI}^0 = 3\omega - IP$.

With the increase of the peak intensity, both the above mentioned main features in the radial density acquire additional multiple-peak sub-structures. This is due to dynamic interference. In the diabatic picture, each peak within the hump represents electrons released during different Rabi cycles. As the photoionization mainly takes place at each half-completed Rabi cycle when the population of the ground state is promoted to the $2p$ excited state (see Fig. 1 in Ref. [9]), the emitted bunches of photoelectrons are separated in time and in space. The peaks in the hump appearing in Fig. 1 at larger distances are emitted at earlier times, and those at smaller distances at later times. Therefore, the number of peaks in the radial density is equal to the number of the Rabi cycles completed during the pulse. Such a multiple-peak sub-structure also persists for the radial density of the ATI electrons. However, due to the partial overlap with the dominant hump, not all sub-peaks are visible in the shoulder.

Fig. 2 depicts on a logarithmic scale the respective total electron spectra, obtained by the Fourier transformation of the spatial wave packets. The lowermost curve in the figure represents, as indicated on its left hand side, the spectrum obtained for the lowest considered peak intensity of the pulse. In this spectrum, the PI electrons with kinetic energy of about $\epsilon_{PI}^0 = 2\omega - IP = 6.8$ eV and the ATI electrons with kinetic energy of about $\epsilon_{ATI}^0 = 3\omega - IP = 17.0$ eV appear as two sharp peaks, as expected in the weak field regime.

Download English Version:

<https://daneshyari.com/en/article/7837152>

Download Persian Version:

<https://daneshyari.com/article/7837152>

[Daneshyari.com](https://daneshyari.com)